ELSEVIER

Nuclear Instruments and Methods in Physics Research A 488 (2002) 332–341

NUCLEAR INSTRUMENTS & METHODS IN PHYSICS RESEARCH Section A

www.elsevier.com/locate/nima

Treatment of multiple scattering with the generalized Riemann sphere track fit

A. Strandlie[a,*], J. Wroldsen[a], R. Frühwirth[b]

[a] *Faculty of Technology, Gjøvik University College, Gjøvik, Norway*
[b] *Institute for High Energy Physics of the Austrian Academy of Sciences, Vienna, Austria*

Received 4 September 2001; received in revised form 3 January 2002; accepted 21 January 2002

Abstract

In this paper, we present a generalization of the Riemann sphere track fitting method. This generalization makes it possible to efficiently include multiple scattering effects in the estimation procedure. We also show that the Riemann fit can be formulated in an alternative way through a mapping to a *paraboloid*. This yields results equivalent to the standard formulation, but with the added advantage that measurements with errors both in $R\Phi$ as well as in the radial direction can be handled in a straightforward manner.

PACS: 07.05.Kf; 11.80.La; 29.85.+c

Keywords: Track fitting; Multiple scattering; Riemann fit; Kalman filter; Global least-squares fit

1. Introduction

The application of least-squares methods in track fitting has a long history in high-energy physics experiments. When the tracks in a collider experiment traverse a detector embedded in a magnetic field, this least-squares problem becomes a non-linear one, even if the field is homogeneous. The non-linearity arises due to the fact that trajectories of charged particles in a homogeneous magnetic field are helical, or, in the bending plane of the particles, circles.

In order to apply linear least-squares methods for circle fitting, the track model or the function describing the relation between the track parameter vector at one detector layer with the track parameter vector at another detector layer has to be linearized. The global least-squares fit [1] and the Kalman filter [2] are widely used methods based on this strategy. In fact, these two methods are equivalent if all correlations due to multiple Coulomb scattering are taken into account in the construction of the covariance matrix of the measurements in the global fit. If this is done properly, the linear least-squares fit is the optimal, linear estimation method. A possible disadvantage of linearized least-squares methods is the requirement of knowing the derivatives of the track parameters at one layer with respect to those at another layer. Such a feature makes these methods non-trivial to implement from scratch in a

*Corresponding author. CERN, EP division, CH-1211 Genève 23, Switzerland.

E-mail addresses: are.strandlie@cern.ch (A. Strandlie), joern.wroldsen@hig.no (J. Wroldsen), fruhwirth@hephy.oeaw.ac.at (R. Frühwirth).

0168-9002/02/$ - see front matter
PII: S0168-9002(02)00465-5

computer program. In addition, approximate track parameters have to be known in advance in order to be able to compute those derivatives.

Another class of circle fits comprises fast and relatively simple methods based on various simplifications of the full, non-linear problem. Traditional approaches belonging to this class are the conformal mapping method [3] and the method due to Karimäki [4]. The conformal mapping method maps circles going through the origin to straight lines and fits the mapped measurements to a straight line, or, in the case of a possibly non-zero impact parameter, a parabola. The Karimäki method is based on finding an exact solution to a slightly modified cost function. A novel development also belonging to this class of circle fit methods is the so-called *Riemann fit* [5]. The Riemann fit maps the measurements onto a Riemann sphere [6] and fits a plane to the transformed, three-dimensional measurements. In the case of negligible multiple scattering, the Riemann fit has been shown to give very accurate estimates of the track parameters [5]. An obvious disadvantage of the above-mentioned, fast methods is that they are not equipped to handle material effects like multiple scattering in an efficient manner. In cases where multiple scattering cannot be neglected, they will therefore not be as precise as the global fit or the Kalman filter.

We will in this paper present a generalization of the Riemann fit method which makes it significantly more precise than methods of the same class and virtually as precise as the Kalman filter in situations with non-negligible multiple scattering. The generalization is a natural extension of the standard formulation of the method, yielding an estimation procedure similar to the original one. Knowledge of the track parameter derivatives is still not required, which in our opinion makes this generalized Riemann fit much simpler to implement than the Kalman filter. It is, of course, less general than the Kalman filter which can operate in arbitrary magnetic fields. On the other hand, it works also for tracks which turn in the magnetic field—a truly disastrous case for the Kalman filter.

We will also show that the Riemann fit can be formulated in an alternative way by mapping the measurements onto a *paraboloid* rather than a Riemann sphere. The resulting fitting procedure yields values of the estimated parameters totally equivalent to those of the standard Riemann fit. It will be shown, however, that the paraboloid fit makes the track parameter error calculations significantly more simple in cases where there are measurement errors also in the radial direction. This is relevant in applications of the Riemann fit in disk style silicon detectors.

Through a simulation experiment in the ATLAS Inner Detector TRT, it will be demonstrated that the generalized Riemann fit is very close to the Kalman filter in precision, even at low momenta. It will also be shown that the generalized Riemann fit is superior to the Karimäki method in the case where multiple scattering is included in the simulations.

The paper is organized as follows. In the next section, we will introduce the paraboloid formulation of the Riemann fit and derive the formulas needed for a concrete implementation of the method. Thereafter, the generalization of the method efficiently incorporating multiple scattering effects will be presented. Finally, we will show results from the simulation experiment in the ATLAS Inner Detector TRT.

2. The paraboloid formulation

The method of fitting tracks by mapping the measurements onto the Riemann sphere has been presented in Ref. [5], and an analysis of the errors of the estimated track parameters can be found in Ref. [7]. Since a detailed description of the method can be found in these two publications, we refer the reader to them for a review.

2.1. Basic properties

Our mapping of a measurement (u_i, v_i) onto a circular paraboloid with minimum point in the origin and symmetry axis along the z-axis is given by

$$x_i = u_i \tag{1}$$

$$y_i = v_i \tag{2}$$

$$z_i = u_i^2 + v_i^2. \tag{3}$$

The transformed point can also be found by the intersection between the vertical line through the point (u_i, v_i) and the paraboloid.

Points (u, v) lying on a circle with radius of curvature ρ and centre coordinates (u_0, v_0) are subject to the relation

$$(u - u_0)^2 + (v - v_0)^2 = \rho^2. \tag{4}$$

Evaluating the expressions inside the brackets and mapping the points (u, v) onto the paraboloid, applying Eqs. (1)–(3), we end up with

$$z - 2v_0 y - 2u_0 x + u_0^2 + v_0^2 - \rho^2 = 0. \tag{5}$$

Points lying on a circle in the uv-plane are thus seen to be mapped onto a plane in space. Therefore, in a fashion similar to the standard Riemann fit, the task of fitting a set of measurements to a circular arc in the uv-plane can be transformed into the task of fitting the measurements mapped onto the paraboloid to a plane in space.

In a similar manner as for the original Riemann fit, the fitted plane is defined by minimizing

$$S = \sum_{i=1}^{N} \frac{(c + n_1 x_i + n_2 y_i + n_3 z_i)^2}{\sigma_i^2} = \sum_{i=1}^{N} \frac{d_i^2}{\sigma_i^2} \tag{6}$$

with respect to c, n_1, n_2 and n_3, i.e. we want to minimize the sum of squared distances d_i^2—properly weighted with the variances σ_i^2 of the measurement errors in the uv-plane—from the mapped measurements to the plane. The number N denotes the number of measurements in the track candidate. Note that in contrast to the standard Riemann fit, there is no radius-dependent weighting of the distances d_i in the cost function. This can be understood by working out the relation between d_i and the corresponding distance in the uv-plane. By doing so, we find that

$$d_i = 2n_3 \rho d_{uv,i} \tag{7}$$

where $d_{uv,i}$ is the distance in the uv-plane from measurement i to the track. Since the distances in space and those in the plane are proportional, the constant of proportionality being the same for all measurements, we may discard it from the cost function S. Minimizing S with respect to the parameters of the plane is therefore equivalent to minimizing the sum of resolution-weighted squared distances from the measurements in the uv-plane to the circle, which is exactly what we want to do.

The procedure of finding the set of parameters $\{c, n_1, n_2, n_3\}$ minimizing S is very similar to that of the standard Riemann fit, since the only difference is in the structure of the weights. Therefore, $\boldsymbol{n}$ must be chosen as the unit eigenvector of the sample covariance matrix $\boldsymbol{A}$ of the measurements,

$$\boldsymbol{A} = \frac{1}{N} \sum_{i=1}^{N} \frac{1}{\sigma_i^2} (\boldsymbol{r}_i - \boldsymbol{r}_{\mathrm{cg}})(\boldsymbol{r}_i - \boldsymbol{r}_{\mathrm{cg}})^{\mathrm{T}} \tag{8}$$

corresponding to the smallest eigenvalue. Furthermore, c is given by

$$c = -\boldsymbol{n}^{\mathrm{T}} \boldsymbol{r}_{\mathrm{cg}} \tag{9}$$

with the centre of gravity vector $\boldsymbol{r}_{\mathrm{cg}}^{\mathrm{T}} = (x_{\mathrm{cg}}, y_{\mathrm{cg}}, z_{\mathrm{cg}})$, where

$$x_{\mathrm{cg}} = \sum_{i=1}^{N} w_i x_i \tag{10}$$

$$y_{\mathrm{cg}} = \sum_{i=1}^{N} w_i y_i \tag{11}$$

$$z_{\mathrm{cg}} = \sum_{i=1}^{N} w_i z_i. \tag{12}$$

In this case, the weights w_i are given as

$$w_i = \frac{1/\sigma_i^2}{\sum_{j=1}^{N} 1/\sigma_j^2}. \tag{13}$$

Knowing that the equation of a plane with unit normal vector $\boldsymbol{n}^{\mathrm{T}} = (n_1, n_2, n_3)$ and signed distance c to the origin is given by $c + n_1 x + n_2 y + n_3 z = 0$, the mapping of the parameters of the plane down to the circle parameters can from Eq. (5) be identified as

$$u_0 = -\frac{n_1}{2n_3} \tag{14}$$

$$v_0 = -\frac{n_2}{2n_3} \tag{15}$$

$$\rho^2 = \frac{1 - n_3^2 - 4cn_3}{4n_3^2}. \tag{16}$$

2.2. Error analysis

The procedure of finding a covariance matrix of the estimated parameters for the fit on the paraboloid is again very similar to that of the standard Riemann fit, as described in Ref. [7]. The covariance matrix of the normal vector can be found in exactly the same manner, and the formulas for the variance of c and the covariances between c and $\boldsymbol{n}$ are still valid. However, there are differences in the calculations of the covariance matrix of the centre of gravity vector $\boldsymbol{r}_{\mathrm{cg}}$ as well as in the linear error propagation from the parameters of the plane to the ordinary circle parameters.

For the paraboloid fit, the easiest way of obtaining a coherent description of the error calculations is to operate with Cartesian coordinates. However, we assume that the relevant detector system has measurement errors in $R\Phi$ (denoted $\sigma_{R\Phi,i}$) and, possibly, measurement errors in R (denoted $\sigma_{R,i}$) uncorrelated to the former. These errors thus need to be transformed into errors in x and y,[1] and this is done by linear error propagation.

We first consider the case of a vanishing error in the radial direction. By straightforward linear error propagation, the following useful relations are easily found:

$$\mathrm{cov}(x_i, x_j) = \sin\Phi_i \sin\Phi_j \,\mathrm{cov}((R\Phi)_i, (R\Phi)_j) \tag{17}$$

$$\mathrm{cov}(x_i, y_j) = -\sin\Phi_i \cos\Phi_j \,\mathrm{cov}((R\Phi)_i, (R\Phi)_j) \tag{18}$$

$$\mathrm{cov}(y_i, y_j) = \cos\Phi_i \cos\Phi_j \,\mathrm{cov}((R\Phi)_i, (R\Phi)_j) \tag{19}$$

with

$$\mathrm{cov}((R\Phi)_i, (R\Phi)_j) = \begin{cases} \sigma^2_{R\Phi,i} & \text{if } i = j \\ 0 & \text{if } i \neq j. \end{cases} \tag{20}$$

Here, Φ_i is the azimuthal angle of the coordinates (x_i, y_i). Since z is assumed to be without any error, the correlations between z and the other coordinates are zero. From the above relations, the covariance matrix of the centre of gravity vector can straightforwardly be derived. The non-zero elements of this are

$$\mathrm{cov}(x_{\mathrm{cg}}, x_{\mathrm{cg}}) = \boldsymbol{w}^{\mathrm{T}} \boldsymbol{C}_{xx} \boldsymbol{w} \tag{21}$$

$$\mathrm{cov}(x_{\mathrm{cg}}, y_{\mathrm{cg}}) = \boldsymbol{w}^{\mathrm{T}} \boldsymbol{C}_{xy} \boldsymbol{w} \tag{22}$$

$$\mathrm{cov}(y_{\mathrm{cg}}, y_{\mathrm{cg}}) = \boldsymbol{w}^{\mathrm{T}} \boldsymbol{C}_{yy} \boldsymbol{w} \tag{23}$$

where $\boldsymbol{w}$ is a vector consisting of the different weights, $\boldsymbol{C}_{xx}$ and $\boldsymbol{C}_{yy}$ are the (diagonal) covariance matrices of the x- and y-coordinate, respectively, and $\boldsymbol{C}_{xy}$ is the (diagonal) correlation matrix of x and y (defined such that the ijth element of this matrix is $\mathrm{cov}(x_i, y_j)$).

In exactly the same spirit, similar relations can be derived for the case of a non-zero measurement error in the radial direction. For the covariances of the different measurements, we obtain

$$\begin{aligned}\mathrm{cov}(x_i, x_j) = {} & \cos\Phi_i \cos\Phi_j \,\mathrm{cov}(R_i, R_j)) \\ & + \sin\Phi_i \sin\Phi_j \,\mathrm{cov}((R\Phi)_i, (R\Phi)_j)\end{aligned} \tag{24}$$

$$\begin{aligned}\mathrm{cov}(x_i, y_j) = {} & \cos\Phi_i \sin\Phi_j \,\mathrm{cov}(R_i, R_j)) \\ & - \sin\Phi_i \cos\Phi_j \,\mathrm{cov}((R\Phi)_i, (R\Phi)_j)\end{aligned} \tag{25}$$

$$\begin{aligned}\mathrm{cov}(y_i, y_j) = {} & \sin\Phi_i \sin\Phi_j \,\mathrm{cov}(R_i, R_j)) \\ & + \cos\Phi_i \cos\Phi_j \,\mathrm{cov}((R\Phi)_i, (R\Phi)_j)\end{aligned} \tag{26}$$

$$\mathrm{cov}(z_i, x_j) = 2(x_i \,\mathrm{cov}(x_i, x_j) + y_i \,\mathrm{cov}(x_j, y_i)) \tag{27}$$

$$\mathrm{cov}(z_i, y_j) = 2(x_i \,\mathrm{cov}(x_i, y_j) + y_i \,\mathrm{cov}(y_i, y_j)) \tag{28}$$

$$\begin{aligned}&\mathrm{cov}(z_i, z_j) \\ &\quad = 4(x_i x_j \,\mathrm{cov}(x_i, x_j) + x_i y_j \,\mathrm{cov}(x_i, y_j) \\ &\qquad + x_j y_i \,\mathrm{cov}(x_j, y_i) + y_i y_j \,\mathrm{cov}(y_i, y_j))\end{aligned} \tag{29}$$

where

$$\mathrm{cov}(R_i, R_j) = \begin{cases} \sigma^2_{R,i} & \text{if } i = j \\ 0 & \text{if } i \neq j. \end{cases} \tag{30}$$

Furthermore, the non-zero elements of the covariance matrix of $\boldsymbol{r}_{\mathrm{cg}}$ are now

$$\mathrm{cov}(x_{\mathrm{cg}}, x_{\mathrm{cg}}) = \boldsymbol{w}^{\mathrm{T}} \boldsymbol{C}_{xx} \boldsymbol{w} \tag{31}$$

$$\mathrm{cov}(x_{\mathrm{cg}}, y_{\mathrm{cg}}) = \boldsymbol{w}^{\mathrm{T}} \boldsymbol{C}_{xy} \boldsymbol{w} \tag{32}$$

$$\mathrm{cov}(y_{\mathrm{cg}}, y_{\mathrm{cg}}) = \boldsymbol{w}^{\mathrm{T}} \boldsymbol{C}_{yy} \boldsymbol{w} \tag{33}$$

$$\mathrm{cov}(z_{\mathrm{cg}}, x_{\mathrm{cg}}) = 2(\boldsymbol{w}^{\mathrm{T}} \boldsymbol{C}_{xx} \boldsymbol{w}_x + \boldsymbol{w}^{\mathrm{T}} \boldsymbol{C}_{xy} \boldsymbol{w}_y) \tag{34}$$

[1] We will in the following make no distinction between the coordinates (u, v) of the plane and the coordinates (x, y) of the paraboloid, since the mapping between them is trivial.

$$\mathrm{cov}(z_{\mathrm{cg}}, y_{\mathrm{cg}}) = 2(\boldsymbol{w}_x^{\mathrm{T}}\boldsymbol{C}_{xy}\boldsymbol{w} + \boldsymbol{w}^{\mathrm{T}}\boldsymbol{C}_{yy}\boldsymbol{w}_y) \tag{35}$$

$$\begin{aligned}\mathrm{cov}(z_{\mathrm{cg}}, z_{\mathrm{cg}}) = 4(&\boldsymbol{w}_x^{\mathrm{T}}\boldsymbol{C}_{xx}\boldsymbol{w}_x + \boldsymbol{w}_x^{\mathrm{T}}\boldsymbol{C}_{xy}\boldsymbol{w}_y \\ &+ \boldsymbol{w}_y^{\mathrm{T}}\boldsymbol{C}_{xy}^{\mathrm{T}}\boldsymbol{w}_x + \boldsymbol{w}_y^{\mathrm{T}}\boldsymbol{C}_{yy}\boldsymbol{w}_y)\end{aligned} \tag{36}$$

where $\boldsymbol{w}_x$ and $\boldsymbol{w}_y$ are vectors whose elements are $(\boldsymbol{w}_x)_i = w_i x_i$ and $(\boldsymbol{w}_y)_i = w_i y_i$, respectively. Note that for the standard Riemann fit, there is a radius-dependent term both in the Riemann sphere coordinates and in the weights. It is this feature which would make the corresponding calculations for the standard Riemann fit more tedious and less coherent than those of the paraboloid fit presented above.

Given the full covariance matrix $\boldsymbol{C}_{(c,\boldsymbol{n})}$ of the estimated parameters on the paraboloid, the covariance matrix of a set of parameters of the original circle parameters will, as in Ref. [7], be evaluated by linear error propagation. If we choose the curvature κ, the impact parameter a_0 and the angle of inclination ψ at the point of closest approach to the origin as our set of parameters,[2] the mapping is given by

$$\psi = \arctan\left(\frac{n_2}{n_1}\right) \tag{37}$$

$$\kappa = s\frac{2n_3}{\sqrt{1 - n_3^2 - 4cn_3}} \tag{38}$$

$$a_0 = s\frac{\sqrt{1 - n_3^2 - 4cn_3} - \sqrt{1 - n_3^2}}{2n_3}. \tag{39}$$

Here s is the product of the sign of κ and the sign of n_3. The non-zero terms of the Jacobian of the transformation from $\{c, \boldsymbol{n}\}$ to $\{\psi, \kappa, a_0\}$ are given as

$$\frac{\partial\psi}{\partial n_1} = -\frac{n_2}{n_1^2 + n_2^2} \tag{40}$$

$$\frac{\partial\psi}{\partial n_2} = \frac{n_1}{n_1^2 + n_2^2} \tag{41}$$

[2] The sign conventions of the parameters are the same as in Ref. [7].

$$\frac{\partial\kappa}{\partial n_3} = s\left(\frac{2}{\sqrt{1 - n_3^2 - 4cn_3}} + \frac{2n_3(2c + n_3)}{(1 - n_3^2 - 4cn_3)^{3/2}}\right) \tag{42}$$

$$\frac{\partial\kappa}{\partial c} = s\frac{4n_3^2}{(1 - n_3^2 - 4cn_3)^{3/2}} \tag{43}$$

$$\begin{aligned}\frac{\partial a_0}{\partial n_3} = s\Bigg(&\frac{\sqrt{1 - n_3^2} - \sqrt{1 - n_3^2 - 4cn_3}}{2n_3^2} + \frac{1}{2\sqrt{1 - n_3^2}} \\ &- \frac{2c + n_3}{2n_3\sqrt{1 - n_3^2 - 4cn_3}}\Bigg)\end{aligned} \tag{44}$$

$$\frac{\partial a_0}{\partial c} = s\frac{-1}{\sqrt{1 - n_3^2 - 4cn_3}}. \tag{45}$$

3. Treatment of multiple scattering

The cost function S, stated in Eq. (6), can be written

$$S = \boldsymbol{d}^{\mathrm{T}}\boldsymbol{G}\boldsymbol{d} \tag{46}$$

where $\boldsymbol{d}$ is a vector consisting of the distances d_i and $\boldsymbol{G}$ is the inverse covariance matrix of the original measurements. Note that this covariance matrix is diagonal, since the effect of multiple scattering is implicitly supposed to be negligible. For particles not having extremely high momenta, even in tracking detectors it is well known that multiple scattering imposes a non-negligible disturbance of the particle trajectories. We therefore propose a generalization of the above cost function in which the covariance matrix $\boldsymbol{G}^{-1}$ is modified in order to contain correlations due to multiple scattering, much in the same spirit as for the global least-squares track fit [8]. We have chosen a simple strategy for the evaluation of this covariance matrix, which implicitly assumes that the tracks are straight [8]. It will be shown in the simulation experiment of the next section that this strategy gives results which are close to optimal, even for tracks with relatively low momenta.

Following the same approach as Regler, the covariances of the errors perpendicular to the track due to multiple scattering are given by

$$\mathrm{cov}((R\Phi)_{\mathrm{ms},k},(R\Phi)_{\mathrm{ms},l}) = \sum_{i=1}^{\min(k-1,l-1)} (R_k - R_i)(R_l - R_i)\frac{\sigma^2_{\phi,i}}{\sin^2(\theta)} \quad (47)$$

where R_i is the radius of detector layer i, $\sigma^2_{\phi,i}$ is the variance of the projected multiple scattering angle in layer i, θ is the polar angle of the track, and the subscript ms denotes multiple scattering. It can be noted that this formula puts no restriction on the particular configuration of the radii of the scattering centres, which means that it works equally well in cases where the scattering centres are less uniformly positioned than in the ATLAS TRT.

The standard deviation $\sigma_{\phi,i}$ of this scattering angle is given by the Highland formula [9]

$$\sigma_{\phi,i} = \frac{0.015}{p}\sqrt{X_i}(1 + 0.038\log(X_i)) \quad (48)$$

where the momentum p of the particle is given in GeV/c and X_i is the number of radiation lengths traversed during the passage of the scattering device. Note that X_i depends on the angle of inclination of the track, so there is an implicit dependence on θ in this quantity. The full covariance matrix used in our approach is the sum of the multiple scattering covariance matrix, whose terms are given in Eq. (47), and the measurement error covariance matrix.

As before, the fitted parameters are found by minimizing S with respect to c and $\boldsymbol{n}$. For $\partial S/\partial c = 0$, we get

$$c = -\boldsymbol{n}^{\mathrm{T}}\boldsymbol{r}_{\mathrm{cg}} \quad (49)$$

where the elements of the centre of gravity vector again can be written as in Eqs. (10)–(12). However, the weights w_j are now given by

$$w_j = \frac{\sum_i (\boldsymbol{G})_{ij}}{\sum_{i,j}(\boldsymbol{G})_{ij}}. \quad (50)$$

Inserting Eq. (49) into the expression of the cost function gives

$$S = \boldsymbol{n}^{\mathrm{T}}\boldsymbol{X}^{\mathrm{T}}\boldsymbol{G}\boldsymbol{X}\boldsymbol{n} \quad (51)$$

where

$$\boldsymbol{X} = \begin{pmatrix} x_1 - x_{\mathrm{cg}} & y_1 - y_{\mathrm{cg}} & z_1 - z_{\mathrm{cg}} \\ \vdots & \vdots & \vdots \\ x_N - x_{\mathrm{cg}} & y_N - y_{\mathrm{cg}} & z_N - z_{\mathrm{cg}} \end{pmatrix}. \quad (52)$$

Also as before, the fitted $\boldsymbol{n}$ is the unit eigenvector of $\boldsymbol{X}^{\mathrm{T}}\boldsymbol{G}\boldsymbol{X}$ corresponding to the smallest eigenvalue of this matrix.

The calculations of the errors of the estimated parameters are almost identical to the procedure of Section 2, and the only difference arises in the evaluation of the covariance matrix of the centre of gravity vector. The necessary modification is to use the full covariance matrix in the evaluation of Eqs. (17)–(19), resulting in $\boldsymbol{C}_{xx}$, $\boldsymbol{C}_{xy}$ and $\boldsymbol{C}_{yy}$ being non-diagonal. Also, the weights w_j as given in Eq. (50) now have to be used in the calculations.

4. A simulation experiment in the ATLAS TRT

We will in this section state results from a simulation experiment in the ATLAS Inner Detector Transition Radiation Tracker (TRT) [10]. Our simulation experiment has been performed in the barrel part of the TRT. We have turned the mirror hits off during the simulations, and we assume that the track finding problem has been completely resolved beforehand. We do this because the main purpose of the experiment is to investigate the effect of the detector material on the accuracy of different algorithms for track fitting. Multiple scattering has been included in the simulations by adding a certain amount of material in each layer with a measurement, this amount being roughly equal to the average amount of material traversed by a particle going through the barrel part of the TRT, which is about 15% of a radiation length, divided by the average number of measurements in the same detector [10]. The range of the polar angle θ of the tracks has been restricted by the requirement that the tracks should stay entirely in the barrel part of the TRT on their way through the detector. It is assumed that the material can be treated as thin layers, i.e. the offset of the track after having penetrated a layer has been set to zero.

We have evaluated the performance of five different methods for track fitting in this simulation study. They are the Kalman filter, the Riemann fit with corrections due to multiple scattering, the Karimäki method using the diagonal terms of the full covariance matrix, a global least-squares fit using the same diagonal terms of the full covariance matrix, and the Kalman filter neglecting multiple scattering. Since the Karimäki method by construction only can handle diagonal terms of multiple scattering, using these is the only way one can try to improve the behaviour of this method in the case of non-negligible scattering. The corresponding global least-squares fit has been included in order to serve as a cross-check of the results obtained by the Karimäki method.

For all of the algorithms, the polar angle of each individual track has been set equal to the true value of this angle. In a real experiment, θ would have to be given by the track finder, which in any case would have to include information from other detectors than the TRT (since the TRT only yields information of hit coordinates in the bending plane). Since we use the same value of θ for all algorithms, no bias in the relative behaviour of the algorithms should be introduced by such a simplification.

Our first investigation has been focusing on the accuracy of the estimated track parameters. In Fig. 1, a plot of the relative generalized variances (with the Kalman filter as baseline) as a function of the transverse momentum p_T of the tracks is shown. We recall that the generalized variance is the determinant of the sample covariance matrix of the residuals of the estimated track parameters with respect to the true track parameters. It turns out that the relative precision of the algorithms for a fixed p_T is virtually independent of the polar angle of the track, and the dependence on θ is therefore not shown. For the results of Fig. 1, $\theta = \pi/2$.

In Table 1, we show the relative standard deviations of the residuals of the estimated track parameters with respect to the true track parameters at $p_T = 1$ GeV/c. The baseline is again the Kalman filter.

As expected, the Kalman filter is the most precise algorithm for the entire p_T range. However, the Riemann fit with multiple scattering corrections is seen to be very close in precision to the

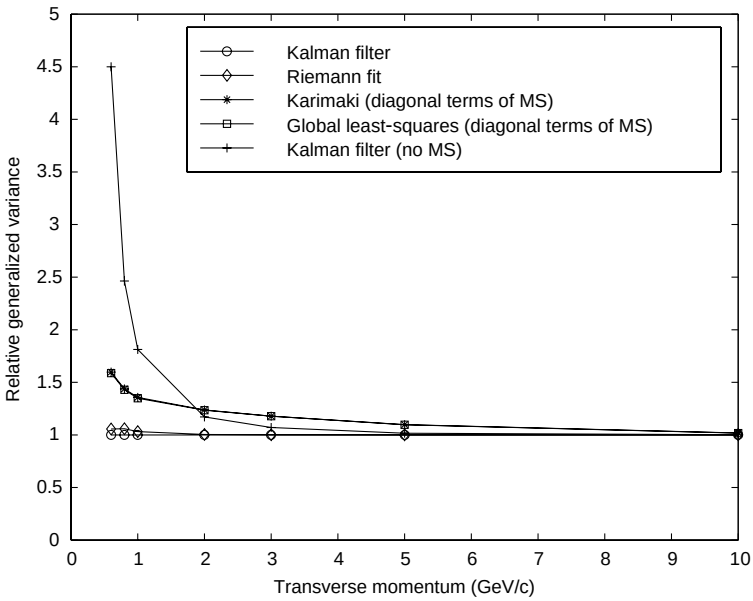

Fig. 1. The relative generalized variance of the five methods as a function of p_T.

Table 1
Relative standard deviations σ_{rel} of the residuals of the estimated parameters ψ, κ and a_0 with respect to the true track parameters at $p_{\mathrm{T}} = 1$ GeV/c

Method	$\sigma_{\mathrm{rel},\psi}$	$\sigma_{\mathrm{rel},\kappa}$	$\sigma_{\mathrm{rel},a_0}$
Kalman filter	1.000	1.000	1.000
Riemann fit	1.015	1.015	1.015
Karimäki (diagonal terms of MS)	1.126	1.141	1.107
Global least-squares (diagonal terms of MS)	1.123	1.138	1.104
Kalman filter (no MS)	1.066	1.045	1.095

Kalman filter, even at relatively low momenta. The Karimäki method and the global least-squares fit are seen to be very close in precision. This is expected, since the two methods are very close to being equivalent. When comparing the Karimäki method and the Kalman filter neglecting multiple scattering, however, we observe that at $p_{\mathrm{T}} = 1$ GeV/c, the Karimäki method is better when considering the generalized variance but worse when considering the individual resolutions of the track parameters. This means that no conclusion can be drawn concerning which of the two

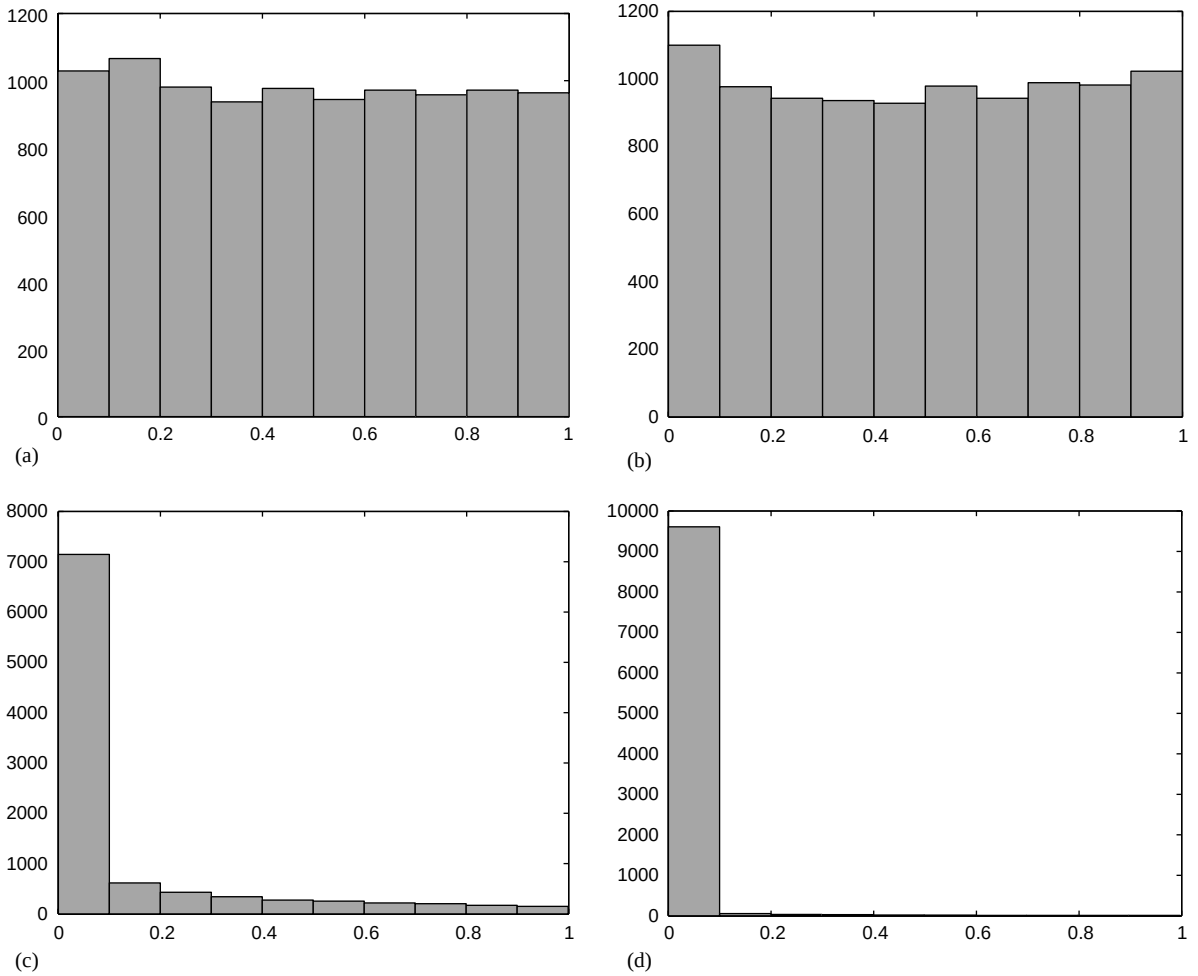

Fig. 2. Histograms of tail probabilities of the Kalman filter (a), the Riemann fit (b), the Karimäki fit (c), and the Kalman filter neglecting multiple scattering (d).

methods is the best. In both cases we use a wrong measurement covariance matrix, and it is not obvious which of the two wrong approaches will be superior. Thus, inclusion of non-diagonal terms of multiple scattering is seen to be indispensible in order to achieve results being close to optimal in precision.

For the different algorithms, we have also studied to which extent the covariance matrices of the estimated parameters reflect the actual spread of the parameters. For this purpose, histograms of the tail probabilities for $p_T = 1\ \mathrm{GeV}/c$ are shown in Fig. 2. (Since the Karimäki method and the global least-squares fit produce equivalent results, we have not plotted the histogram of the latter method.) It can be seen that the Kalman filter and the Riemann fit are able to reproduce these errors in a satisfactory manner, whereas the Karimäki fit and the Kalman filter neglecting multiple scattering are not. As can be seen from the probability histogram for the Karimäki fit, also for the error estimates it is obviously not sufficient to include the diagonal terms of multiple scattering—the correlations again have to be included in order to obtain reliable results.

We will also state an expression of the χ^2 of the fitted tracks for the Riemann fit. Recalling the relation given in Eq. (7), the quantity

$$\chi^2_{\mathrm{track}} = \frac{\kappa^2}{4n_3^2}\boldsymbol{d}^{\mathrm{T}}\boldsymbol{G}\boldsymbol{d} \tag{53}$$

should be approximately χ^2-distributed with $N-3$ degrees of freedom. In Fig. 3, we show a plot of the corresponding tail probability histogram of χ^2_{track} for $p_T = 1\ \mathrm{GeV}/c$. Indeed, χ^2_{track} seems to be χ^2-distributed to a satisfactory degree of accuracy.

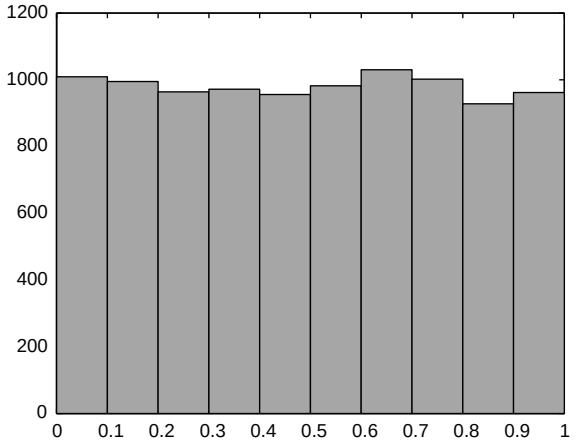

Fig. 3. Histogram of the tail probabilities of χ^2_{track} for $p_T = 1\ \mathrm{GeV}/c$.

5. Conclusions

We have in this paper presented a generalization of the Riemann sphere track fit which enables it to efficiently treat situations where multiple scattering cannot be neglected. We have also shown that the Riemann fit can be formulated through a mapping to a paraboloid rather than to a Riemann sphere. This alternative formulation makes the calculations of the errors of the estimated track parameters simpler in cases where there are measurement errors in the radial direction.

Through a simulation experiment in the ATLAS TRT, the generalized Riemann fit has been shown to be virtually as precise as the Kalman filter for a large range of track momenta. It has also been shown to be more precise than methods either approximately incorporating multiple scattering effects or not incorporating them at all. Moreover, the errors of the estimated parameters of the generalized Riemann fit have been shown to reproduce the actual errors of the parameters in a satisfactory manner.

References

[1] R. Frühwirth, M. Regler, R.K. Bock, H. Grote, D. Notz, Data Analysis Techniques for High-Energy Physics, 2nd Edition, Cambridge University Press, Cambridge, 2000.
[2] R. Frühwirth, Nucl. Instr. and Meth. A 262 (1987) 444.
[3] M. Hansroul, H. Jeremie, D. Savard, Nucl. Instr. and Meth. A 270 (1988) 498.
[4] V. Karimäki, Nucl. Instr. and Meth. A 305 (1991) 187.
[5] A. Strandlie, J. Wroldsen, R. Frühwirth, B. Lillekjendlie, Comput. Phys. Commun. 131 (2000) 95.
[6] L.V. Ahlfors, Complex Analysis: an Introduction to the Theory of Analytic Functions of One Complex Variable,

International Series in Pure and Applied Mathematics, McGraw-Hill, New York, 1979.
[7] A. Strandlie, R. Frühwirth, Nucl. Instr. and Meth. A 480 (2002) 732.
[8] M. Regler, Multiple scattering in least squares fitting, in: R. Bock, et al. (Eds.), Formulae and Methods in Experimental Data Evaluation, Vol. 2, CERN, Geneva, 1984, pp. G1–G11.
[9] D.E. Groom, et al., Eur. Phys. J. C 15 (2000) 1.
[10] ATLAS Inner Detector Technical Design Report, CERN/LHCC 97-16, CERN, Geneva, 1997.